



Light transmission in nanocellular polymers: Are semi-transparent cellular polymers possible?



S. Pérez-Tamarit*, B. Notario, E. Solórzano, M.A. Rodríguez-Perez

CellMat Laboratory, University of Valladolid, Paseo de Belén 7, 47011 Valladolid, Spain

ARTICLE INFO

Article history:

Received 25 July 2017

Received in revised form 24 August 2017

Accepted 26 August 2017

Available online 30 August 2017

Keywords:

Polymers

Poly (methyl methacrylate)

Light transmission

Nanocellular foams

Porous materials

ABSTRACT

This work presents the light transmission through a collection of solid cellular polymers based on poly (methyl methacrylate) (PMMA) with cells sizes covering the micro and nano-scale. The obtained results showed that the behavior of light transmission when cell size is in the nano-scale is opposite to the one shown by microcellular foams or the one predicted by theoretical models of light scattering (LS). In fact, the expected trend is that a reduction of cell size increases the opacity of the samples. However, for nanocellular polymers based on amorphous polymers reducing the cell size increases the light transmission. Therefore, this result indicates that a further reduction of the cell size could result in cellular polymers optically semi-transparent.

© 2017 Elsevier B.V. All rights reserved.

1. Introduction

Nano-cellular polymers represent a new kind of materials which have attracted the attention of the scientific community in the last years due to their surprising properties [1,2]. Nowadays, some papers have been published on the thermal [3], acoustical [4], mechanical [5] or dielectric [6] properties of these materials showing promising results. However, the optical properties of these materials have been less considered [7].

Moreover, similar materials as those studied in this work are silica aerogels [8]. An aerogel is an open-celled, meso-porous, solid cellular material that is composed of a network of interconnected nanostructures. It exhibits a porosity (non-solid volume) greater than 50% and cells with sizes in the nano-scale (ca. 50 nm) [9]. These materials have a combination of properties that no other cellular material possesses simultaneously [10]. For instance, silica aerogels have very low densities and thermal conductivities (Knudsen effect), among other extraordinary properties [11,12]. In addition, these materials, produced from transparent solid matrix (silica) and with pores in the nano-scale, are almost transparent to light in the optical wavelength range (400–750 nm) [9].

Therefore the aim of this paper is to study the optical properties of nanocellular polymers produced from an amorphous polymer (PMMA) trying to elucidate if reducing the cell size to the nanoscale could induce some transparency in the materials. To this

end light transmission (T) through samples has been measured. This property characterizes the transparency of the materials. Transmissivity (T) is defined as the ratio between transmitted (I) and incident (I_0) intensity reaching the light detector (Eq. (1)).

$$T = I/I_0 \quad (1)$$

2. Experimental part

2.1. Materials

The PMMA was kindly provided by Altuglas-Arkema Company (France) in the form of pellets. The material used presents a glass transition temperature (T_g) of 115 °C, density (ρ_s) of 1180 kg/m³ and due to its amorphous structure a high transparency.

2.2. Samples production

PMMA pellets were first dried in a vacuum furnace (680 mmHg) at 80 °C during 4 h. Then, the pellets were molded into precursors of 155 × 75 × 4 mm³ by using a two-hot plate press. The temperature of the press was fixed at 250 °C. The material was molten without pressure for 9 min, then it was compacted under a constant pressure of 21.8 bar for another minute and finally it was cooled under the same pressure.

Foaming experiments were performed in a pressure vessel (PARR4681, Parr Instrument Co.). The pressure system comprises an accurate pressure pump controller (SFT-10, Supercritical Fluid

* Corresponding author.

E-mail address: saúl.perez@fmc.uva.es (S. Pérez-Tamarit).

Table 1
Labels, cell size (ϕ) density (ρ) and relative density (ρ_r) of samples under study.

Sample	ϕ (nm)	ρ (kg/m ³)	ρ_r
Nano-1	25	625.4	0.53
Nano-2	90	568.9	0.48
Nano-3	200	531.5	0.45
Nano-4	350	508.1	0.43
Nano-5	400	519.2	0.44
Micro-1	820	623.3	0.53
Micro-2	1080	638.6	0.54
Micro-3	7000	592.8	0.50
Micro-4	11000	649.0	0.55

Technologies Inc.). The vessel is equipped with a clamp heater (1200 W) controlled via a CAL3300 temperature controller. Therefore, a collection of experiments were implemented following the solid state foaming process [3,13]. The pressure and temperature were selected in order to produce four samples with cells in the micrometer range ($\phi > 500$ nm) and five materials with cells in the nano-scale ($\phi < 500$ nm). The analyzed foamed specimens ($12 \times 12 \times 1$ mm³) were prepared by using a precision buzz saw.

2.3. Characterization techniques

Density of the samples was measured by the water-displacement method using the density determination kit for an AT261 Mettler-Toledo balance. Relative density (ρ_r) is calculated as the ratio between cellular material density (ρ_f) and solid polymer density (ρ_s) resulting for all analyzed samples values close to 0.5 (Table 1). Although the effect of sample density is corrected in transmissivity theoretical models, comparing samples with similar densities is crucial to obtain accurate conclusions.

Cellular structure was determined using a scanning electron microscope (JSM820, Jeol and Quanta 200FEG). Samples were cooled in liquid nitrogen, fractured and finally coated with gold using a sputter coater (SCD005, Blazers Union) for the microscopic visualization. Microscopy images were analyzed using a self-developed application [14] based on ImageJ/Fiji image analysis software [15].

Microcellular materials with cell sizes between 1 and 11 μ m have been selected (Fig. 1 right). The nanocellular samples have cell sizes ranging 25–400 nm (Fig. 1 left). Therefore, three orders of magnitude of difference between the materials with the largest and the smallest cell sizes.

2.4. Experimental set-up for transmissivity measurements

The experimental set-up to measure the light transmission by using Eq. (1) is shown in Fig. 2. The device consist of a photodiode joined to an integrating sphere with 12.5 mm window (PRW0505,

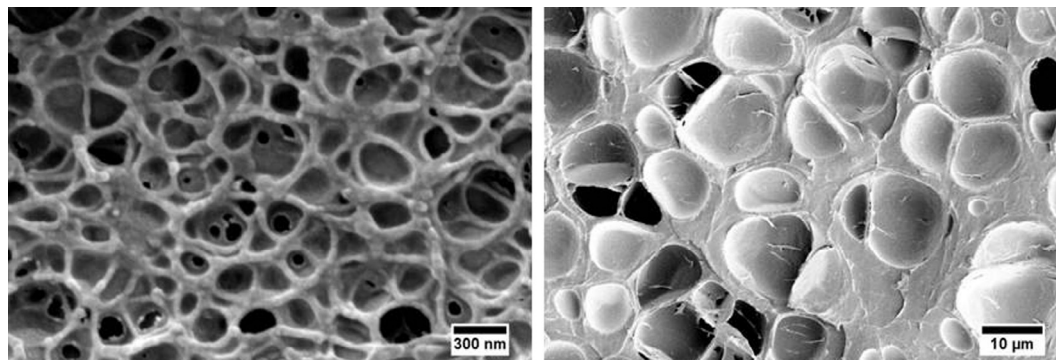


Fig. 1. Micrographs of the two kinds of samples. Nanocellular (25–400 nm) – left- and microcellular (0.8–11 μ m) – right-. Samples are Nano-3 and Micro-4.

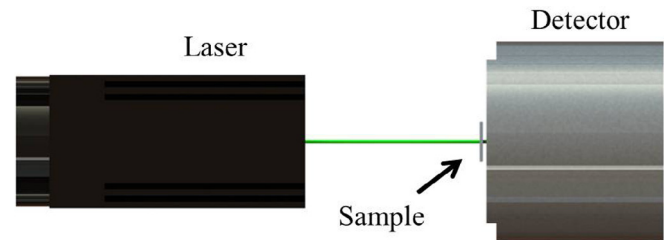


Fig. 2. Sketch of the experimental set-up for transmissivity measurements.

Gigahertz-Optik) connected to a photometer (X94, Gigahertz-Optik) as light detector and three different lasers as light source. The lasers (blue -450 nm-, green -532 nm- and red -650 nm-, 10 mW) were selected in order to investigate the influence of light wavelength in transmission. The samples were placed at a distance less than 1 mm of the detector window and due to their surface ($\sim 12 \times 12$ mm²) and their thickness (~ 1 mm) the totality of light crossing the sample reaches the detector. The laser-detector distance was 30 mm fixing the size of the laser beam at the samples surface (2 mm).

3. Theory

Light scattering models concerning transmission in porous media with a non-absorbing liquid matrix establish that transmissivity is related with sample thickness (L) and transport mean free path of light in the medium (l^*) as long as the mean cell size is much larger than light wavelength (Eq. (2)) [16]. This condition is accomplished by the analyzed microcellular materials but not in the case of nanocellular materials.

$$T \propto l^*/L \quad (2)$$

Mean free path is the average distance a photon travels before its direction is randomized and is related with mean cell size and relative density (Eq. (3)) [17].

$$l^* = \phi/\sqrt{\rho_r} \quad (3)$$

Combining the previous expressions it is possible to define a normalized transmissivity (T_N) that includes the influence of sample thickness and density (Eq. (4)).

$$T_N = LT\sqrt{\rho_r} \quad (4)$$

4. Results

The transmissivity values for the solid material ($\rho_r=1$) were around 0.85 for the three selected lasers. Consequently, PMMA

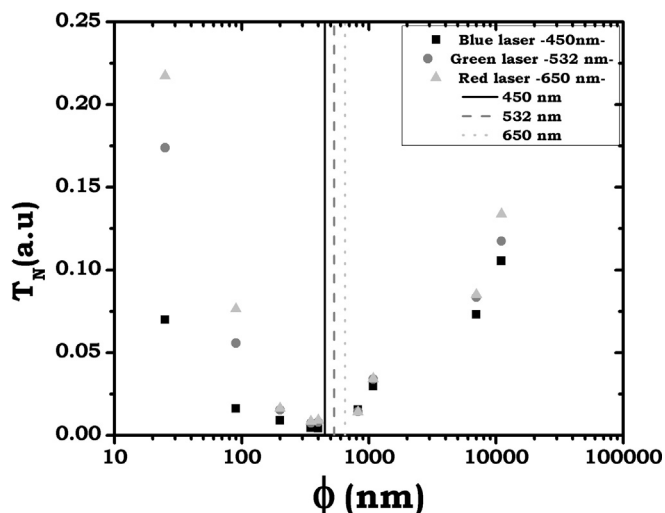


Fig. 3. Normalized transmissivity versus the cell size of the tested samples. Vertical lines correspond to the wavelength of lasers –450, 532 and 650 nm–

polymer is a good candidate in order to manufacture semi-transparent nanofoams.

The normalized transmissivity obtained using different laser beams is represented as a function of mean cell size of the samples (Fig. 3). Two opposite trends are visible. On the one hand, for microcellular foams as the mean pore is reduced the normalized transmissivity decreases. This is the expected behavior for a microcellular material (Eq. (3)). Under these conditions, considering a one-dimensional cellular material, the lower is the cell size; the higher is the solid barriers (cell walls or edges) inside the material. Consequently, the number of light interactions with solid-gas interfaces of the material increases and the amount of light crossing the sample is smaller.

On the other hand, the results show an opposite trend for nanocellular polymers. In this case, a reduction of the cell size causes a significant increment of the transmissivity. In this range of cell sizes, still considering one-dimensional cellular materials, the frequency of solid barriers is higher than the frequency of oscillation of light. This is a possible explanation of the phenomena observed in the figure. As the mean cell size of the cellular material decreases, the interaction of light with the solid-gas interfaces of the foamed samples also decreases resulting in a higher transmissivity. Moreover, in this range of cell sizes the light wavelength influences the transmissivity response, reinforcing the possible explanation presented above that assumes the dependence of transmissivity on the relationship between the cell size and the spatial frequency of light.

Finally, the minimum of the curves (Fig. 3) appears for mean pore sizes close to the light wavelength. However, the lack of samples with cell size in this range prevents knowing the exact minimum of the curves.

5. Conclusions

In summary, the paper presents the first experimental data on the light transmission of nanocellular polymers produced from

an amorphous polymer. The results showed that reducing the cells below the wavelength of the light used in the experiments modifies the trend in the transmissivity versus cell size curve. The tendency is opposite to that observed for materials with cells in the micro-scale or to that predicted by LS models. The results obtained seem to indicate that by further reducing the size of the cells cellular polymers with a significant transparency could be produced.

Further work is required to evaluate this effect for the infrared wavelength range due to its influence on the thermal conductivity of these materials.

Acknowledgments

Financial assistance from MINECO and FEDER program (MAT2012-34901) MINECO, FEDER, UE (MAT2015-69234-R) and the Junta de Castile and Leon (VA011U16) are gratefully acknowledged. Predoctoral contract of S. Pérez-Tamarit by University of Valladolid and Banco Santander (E-47-2015-0094701) is acknowledged.

References

- [1] S. Costeux, CO₂-blown nanocellular foams, *J. Appl. Polym. Sci.* 131 (2014) 41293.
- [2] B. Notario, J. Pinto, M.A. Rodríguez-Pérez, Nanoporous polymeric materials: a new class of materials with enhanced properties, *Prog. Mater. Sci.* 78–79 (2016) 93–139.
- [3] B. Notario, J. Pinto, E. Solorzano, J.A. de Saja, M. Dumon, M.A. Rodríguez-Pérez, Experimental validation of the Knudsen effect in nanocellular polymeric foams, *Polymer* 56 (2015) 57–67.
- [4] B. Notario, A. Ballesteros, J. Pinto, M.A. Rodríguez-Pérez, Nanoporous PMMA: a novel system with different acoustic properties, *Mater. Lett.* 168 (2016) 76–79.
- [5] B. Notario, J. Pinto, M.A. Rodríguez-Pérez, Towards a new generation of polymeric foams: PMMA nanocellular foams with enhanced physical properties, *Polymer* 63 (2015) 116–126.
- [6] B. Notario, J. Pinto, R. Verdejo, M.A. Rodríguez-Pérez, Dielectric behavior of porous PMMA: from the micrometer to the nanometer scale, *Polymer* 107 (2016) 302–305.
- [7] H. Yokoyama, L. Li, T. Nemoto, K. Sugiyama, Tunable nanocellular polymeric monoliths using fluorinated block copolymer templates and supercritical carbon dioxide, *Adv. Mater.* 16 (2004) 1542–1546.
- [8] R. Vacher, T. Woignier, J. Pelous, E. Courtens, Structure and self-similarity of silica aerogels, *Phys. Rev. B* 37 (1988) 6500–6503.
- [9] G.M. Pajonk, Transparent silica aerogels, *J. Non-Cryst. Solids* 225 (1998) 307–314.
- [10] A. Soleimani Dorcheh, M.H. Abbasi, Silica aerogel; synthesis, properties and characterization, *J. Mater. Process. Tech.* 199 (2008) 10–26.
- [11] J.E. Fesmire, Aerogel insulation systems for space launch applications, *Cryogenics* 46 (2006) 111–117.
- [12] R.W. Pekala, J.C. Farmer, C.T. Alviso, T.D. Tran, S.T. Mayer, J.M. Miller, B. Dunn, Carbon aerogels for electrochemical applications, *J. Non-Cryst. Solids* 225 (1998) 74–80.
- [13] A.V. Nawaby, Y.P. Handa, X. Liao, Y. Yoshitaka, M. Tomohiro, Polymer-CO₂ systems exhibiting retrograde behavior and formation of nanofoams, *Polym. Int.* 56 (2007) 67–73.
- [14] J. Pinto, E. Solorzano, M.A. Rodríguez-Pérez, J.A. de Saja, Characterization of the cellular structure based on user-interactive image analysis procedures, *J. Cell. Plast.* 49 (2013) 555–575.
- [15] M.D. Abràmoff, P.J. Magalhaes, J. Sunanda, Image Processing with ImageJ, *Biophotonics Int.* 11 (2004) 36–42.
- [16] D.J. Durian, D.A. Weitz, D.J. Pine, Multiple light-scattering probes of foam structure dynamics, *Science* 252 (1991) 686–688.
- [17] M.U. Vera, A. Saint-Jalmes, D.J. Durian, Scattering optics of foam, *Appl. Opt.* 40 (2001) 4210–4214.